

# Degrees of Freedom of Y Channel with Single-Antenna Users: Transmission Scheme and Beamforming Optimization

Wei Long<sup>1</sup>, Hui Gao<sup>1</sup>, Tiejun Lv<sup>1</sup> and Chau Yuen<sup>2</sup>

<sup>1</sup>Key Laboratory of Trustworthy Distributed Computing and Service, Ministry of Education  
School of Information and Communication Engineering  
Beijing University of Posts and Telecommunications, Beijing, China 100876

[e-mail: {longwei, huigao, lvtiejun}@bupt.edu.cn]

<sup>2</sup>Singapore University of Technology and Design  
20 Dover Drive, Singapore 138682

[e-mail: yuenchau@sutd.edu.sg]

\*Corresponding author: Tiejun Lv

*Received July 10, 2014; revised September 25, 2014; accepted October 14, 2014; published December 31, 2014*

---

## Abstract

In this paper, we investigate the degrees of freedom (DOF) of the Y channel consisting of three single-antenna users and a two-antenna common access relay, where each user intends to exchange independent messages with the other two users with the assistance of the relay. We show that the DOF of this particular scenario is 1.5. In order to prove this result, we firstly derive a DOF upper bound based on cut-set bound by allowing cooperation among users, which shows that the total DOF is upper bounded by 1.5. Then we propose a novel transmission scheme based on asymmetric signal space alignment (ASSA) to demonstrate the achievability of the upper bound. Theoretical evaluation and numerical results confirm that the upper bound can be achieved by utilizing ASSA, which also proves the optimality of the ASSA-based scheme in terms of DOF. Combining the upper bound and achievability, we conclude that the exact DOF is 1.5. Moreover, we present a novel iterative joint beamforming optimization (I-JBO) algorithm to further improve the sum rate. Numerical simulations have been provided to demonstrate the convergence speed and performance advantage of the I-JBO algorithm.

---

**Keywords:** Degrees of freedom, Y channel, single-antenna users, asymmetric signal space alignment, beamforming optimization

---

This paper was presented in part at the 2013 IEEE International Conference on Communications (ICC), Budapest, Hungary. While the preliminary version provided an asymmetric signal space alignment (ASSA) based transmission scheme to investigate the achievable degrees of freedom (DOF) for the Y channel with single-antenna users, the extended version includes the following new contributions: (1) we prove that the exact DOF of the considered scenario is 1.5; (2) we propose an iterative joint beamforming optimization (I-JBO) algorithm to further improve the sum rate. In addition, all sections are revised to improve the presentation and clarity. This work is financially supported by the National Natural Science Foundation of China (NSFC) (Grant No. 61271188, 61401041) and the Fundamental Research Funds for the Central Universities (Grant No. 2014RC0106), and by Singapore University of Technology and Design (SUTD).

<http://dx.doi.org/10.3837/tiis.2014.12.004>

## 1. Introduction

The rapidly increasing demands for wireless multimedia services have promoted the development of novel signaling techniques with high spectrum efficiency [1, 2, 3]. Multiple-input multiple-output (MIMO) and relay are two outstanding representatives of these techniques [4, 5]. By combining MIMO and relay, MIMO two-way relaying channel (TWRC) has been an attractive topic for the reason that it remarkably increases the spectral efficiency of relaying system [6, 7, 8, 9]. Furthermore, the TWRC has been extended into multi-way relay channel (MWRC), which has been considered as a fundamental building block for future cooperative communication systems [10]. In particular, a novel MWRC system model termed MIMO Y channel has been introduced in [11], where each of the three users intends to exchange independent messages with the other two users via an intermediate relay. The authors also proposed a so called signal space alignment (SSA) scheme, which exploits the idea of interference alignment (IA) [12] and network coding (NC) [13, 14]. The information exchange is implemented within only two phases, namely the multiple access (MAC) phase and the broadcast (BC) phase. During the MAC phase, the users cooperatively design their precoding vectors to align the paired signals into the same spatial dimension at the relay, and then all the users transmit to the relay simultaneously. During the BC phase, the relay broadcasts the composite signal back to the users, and then the users extract the useful signals by self-interference cancellation.

As a typical representative of the MWRC, MIMO Y channel can model various communication scenarios and may play an important role in practical wireless systems [10]. Therefore, MIMO Y channel has attracted significantly growing interests. The basic MIMO Y channel has been further extended to the four-user case and the  $K$ -user case in [15] and [16] respectively, where the achievable degrees of freedom (DOF) are investigated. Moreover, some specific problems on MIMO Y channel, such as beamforming design, constellation mapping, diversity techniques, and user scheduling, have been studied in [17, 18, 19, 20]. On the other hand, a special case of the basic Y channel where all the three nodes have a single antenna has been studied in [16] and [21], where insightful results regarding the achievable DOF and the system capacity are obtained. More specifically, the algorithm in [16] is tailored for the single-input single-output (SISO) case. Moreover, the authors have not proved that the algorithm can achieve the DOF upper bound. Therefore, the exact DOF of the basic Y channel with single-antenna users remains an open problem.

In this paper, we study the DOF of the Y channel composed of three single-antenna users and a two-antenna common access relay as shown in Fig. 1. The channel model is practical since it can find many interesting applications in various ad-hoc systems. For example, in a clustered wireless sensor networks (WSN) with three users in each cluster, each sensor may want to share information with its two partners in the same cluster, while the data fusion center can play the role of the relay. Usually, the sensors are constrained by limited size and short battery life, hence multiple antennas may be unrealistic for them. Although the relay usually has greater capability, it is still restricted by the energy limited nature of WSN [22, 23]. Therefore, two antennas may be a reasonable assumption for the relay. For the considered scenario, we first derive the DOF upper bound. Then we study the transmission scheme to achieve the upper bound. According to the literatures [11, 16], the SSA scheme has been proved to significantly improve the achievable DOF of Y channel, therefore it has the potential to achieve the upper bound. However, according to [11], the traditional SSA is not applicable

in this channel model for the lack of spatial dimensions. Symbol extension enables the application of SSA into the scenario by using the dimensions in time domain. Nevertheless, the symbol extension will cause delay to the network. It is noted that the asymmetric complex signaling (ACS) has been proposed in [24] to provide extra dimensions, which enables IA in the interference channel with single-antenna users. Enlightened by this, we investigate the application of ACS in Y channel and propose a novel asymmetric signal space alignment (ASSA) based scheme tailored for this special scenario, which achieves the DOF upper bound without symbol extension.

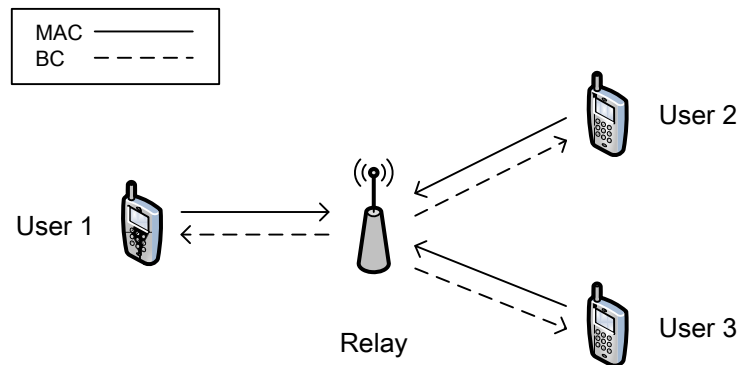


**Fig. 1.** A system diagram for the addressed communication scenario

Beamforming optimization is another hot topic in Y channel, because the performance of the transmission scheme is closely related with the beamforming design. In [19], a random beamforming vector selection approach is proposed to obtain the spatial diversity. Noting that the random selection method can hardly guarantee the optimality, [17] has proposed a deterministic iterative beamforming optimization as well as power allocation scheme to maximize the effective signal to noise ratio (SNR) for each channel realization. Furthermore, [18] has extended the algorithm in [17] into the Y channel with multiple data streams per message. However, the aforementioned algorithms are effective only when the dimension of the intersection space of each user pair is more than one, which doesn't hold in the considered scenario. In order to tackle this difficulty, we propose an efficient beamforming optimization algorithm without the restriction on spatial dimensions.

This paper is an extension of the conference version in [25]. We investigate the DOF and beamforming optimization problems for the Y channel with single-antenna users. To be more specific, the main contributions of this paper are summarized as follows.

1. The exact DOF of the addressed scenario is obtained as 1.5. We draw this conclusion based on the DOF upper bound and achievability. To begin with, the upper bound is derived based on cut-set bound by allowing user cooperation.
2. To confirm the achievability of the upper bound, we propose a novel ASSA-based transmission scheme for this special scenario. At first, we employ ACS to transform the complex system into an equivalent real system with double dimensions. As a result, we can design precoding vectors for each user by utilizing the extra dimensions brought by ACS. Nevertheless, we still cannot align each pair of signals due to excessive dimensions at the relay. To solve this problem, we carefully design a projection matrix at the relay, which projects the received signal into a subspace with appropriate dimensions for ASSA. Then we can apply ASSA into the real system. According to the theoretical evaluation and numerical results, the proposed

ASSA-based scheme obtains 1.5 DOF, which is exactly the upper bound. This result also guarantees the optimality of the ASSA-based scheme in terms of DOF.

3. In order to improve the sum rate, we present an iterative joint beamforming optimization (I-JBO) algorithm. More specifically, we first formulate the beamforming design as a joint optimization problem, which is difficult to solve due to the high computational load. Then we carefully study the coupling part of all the variables and introduce an intermediate variable to express them. Consequently the original beamforming design problem reduces to an equality constrained optimization problem with only one variable vector. Then a heuristic yet effective method, which combines the penalty function method and quasi-Newton method [26], is proposed to obtain a local solution iteratively. More specifically, we first employ penalty function method to convert the original optimization problem into an unconstrained problem. Then the quasi-Newton method is utilized to solve the problem iteratively. Numerical results reveal that the I-JBO algorithm significantly enhances the sum rate.

The remainder of this paper is organized as follows. Section 2 introduces the system and signal models for the addressed communication scenario. In section 3, we derive a DOF upper bound of this channel. In section 4, we present the ASSA scheme in detail to prove the achievability of the upper bound. In section 5, the I-JBO algorithm is introduced to boost the sum rate. The simulation result is given in section 6, followed by some concluding remarks in section 7.

*Notations:* We use bold upper and lower case letters to represent matrices and vectors, respectively. For any matrix  $\mathbf{A}$ ,  $\|\mathbf{A}\|_F$ ,  $\text{tr}(\mathbf{A})$ ,  $\mathbf{A}^H$ ,  $\mathbf{A}^T$ , and  $\mathbf{A}^\dagger$  denote the Frobenius norm, trace, conjugate transpose, transpose, and pseudo inverse of  $\mathbf{A}$ , respectively. For any complex number  $a$ ,  $\text{Re}(a)$ ,  $\text{Im}(a)$  and  $|a|$  denote the real part, imaginary part and modulus of  $a$ , respectively.  $\mathbb{E}\{\cdot\}$  is the expectation operator.  $\|\cdot\|$  and  $\langle \cdot \rangle$  indicate the 2-norm operator and normalization operator for vectors, respectively.  $\text{diag}(a, b, \dots)$  denotes a diagonal matrix with  $\{a, b, \dots\}$  as its diagonal elements.  $\mathbf{R}$  and  $\mathbf{C}$  indicate the set of real and complex numbers, respectively.

## 2. System Model

As shown in Fig. 1, we consider a three-user Y channel where each user  $S_i$ ,  $i=1,2,3$ , has a single antenna, the amplified-and-forward (AF) relay  $R$  is equipped with two antennas, and all the nodes operate in half-duplex mode<sup>1</sup>. Every user intends to send independent messages to the other two users via the relay. The direct links between users are ignored on account of severe fading and path loss. For ease of exposition, we adopt time division duplexing (TDD) system where channel reciprocity holds, therefore the channels for links  $S_i \rightarrow R$  and  $R \rightarrow S_i$  are expressed as  $\mathbf{h}_i \in \mathbf{C}^{2 \times 1}$  and  $\mathbf{h}_i^T \in \mathbf{C}^{1 \times 2}$ , respectively. We also assume flat Rayleigh fading, then the entries of  $\mathbf{h}_i$  are independent and identically distributed (i.i.d.) as  $CN(0,1)$ . Furthermore, perfect global channel state information (CSI) is assumed at all the nodes. The

<sup>1</sup> In fact, all the nodes are assumed to work at full-duplex mode in [16], while we have assumed half-duplex mode in our system model. Because the full-duplex system can transmit and receive signals simultaneously, its achievable DOF is twice of the half-duplex counterpart. In other words, if the half-duplex mode is assumed for the system model in [16], the achievable DOF of their algorithm is only 1.

exchange of network information flow completes in two phases, namely the MAC phase and the BC phase.

During the MAC phase, all the users transmit to  $R$  simultaneously. The received signal at  $R$  is given by

$$\mathbf{y}_R = \sum_{i=1}^3 \mathbf{h}_i x_i + \mathbf{n}_R, \quad (1)$$

where  $x_i \in \mathbf{C}$  is the transmit complex symbol from  $S_i$ , and  $\mathbf{n}_R \in \mathbf{C}^{2 \times 1}$  denotes the additive white Gaussian noise (AWGN) vector with i.i.d. elements following  $CN(0, \sigma_R^2)$ .  $x_i$  is subject to an average power constraint as  $E\{x_i^2\} \leq P_i$ , where  $P_i$  is the transmit power of  $S_i$ .

During the BC phase, the signal transmitted by  $R$  is

$$\mathbf{x}_R = \mathbf{G} \mathbf{y}_R, \quad (2)$$

where  $\mathbf{G} \in \mathbf{C}^{2 \times 2}$  is the processing matrix with the power restriction as  $E\{\text{tr}(\mathbf{G} \mathbf{y}_R \mathbf{y}_R^H \mathbf{G}^H)\} \leq P_R$ .

Consequently,  $S_i$  observes the received signal as

$$y_i = \mathbf{h}_i^T \mathbf{x}_R + n_i, \quad (3)$$

where  $n_i \in \mathbf{C}$  denotes the AWGN following  $CN(0, \sigma_i^2)$ , and  $S_i$  tries to extract the useful message from  $y_i$ . For simplicity, we assume equal power allocation and set  $P_i = P_R = P$  and  $\sigma_i^2 = \sigma_R^2 = N_0$ .

DOF is often utilized to characterize the capacity behavior in high SNR regimes. We define the total DOF of the above Y channel as

$$\begin{aligned} d &= \lim_{\rho \rightarrow \infty} \frac{R(\rho)}{\log(\rho)} \\ &= \sum_{i=1}^3 \sum_{j=1, j \neq i}^3 \lim_{\rho \rightarrow \infty} \frac{R_{j,i}(\rho)}{\log(\rho)} \\ &= \sum_{i=1}^3 \sum_{j=1, j \neq i}^3 d_{j,i}, \end{aligned} \quad (4)$$

where  $\rho$  denotes the transmit SNR and is defined as  $\rho = P/N_0$ ,  $R(\rho)$  stands for the sum rate with respect to  $\rho$ ,  $R_{j,i}(\rho)$  is the rate of the link from  $S_i$  to  $S_j$ , and  $d_{j,i} = \lim_{\rho \rightarrow \infty} \frac{R_{j,i}(\rho)}{\log(\rho)}$  denotes the DOF of the link from  $S_i$  to  $S_j$ .

### 3. An Upper Bound on DOF

In this section, we derive an upper bound on the DOF of the considered scenario, which serves as a guideline for the design of transmission scheme.

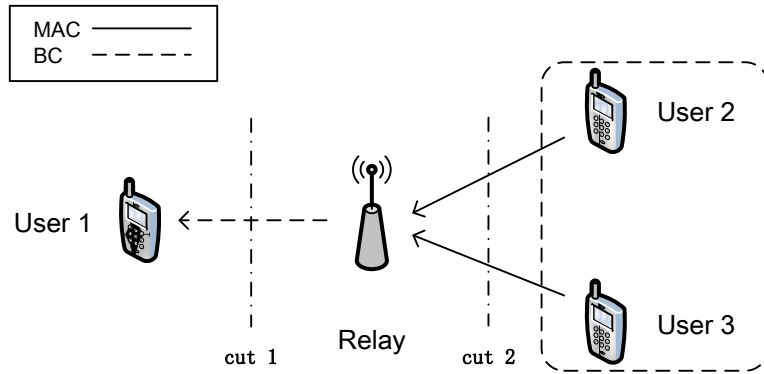


**Fig. 2.** The network information flow from  $\{S_2, S_3\}$  to  $S_1$

**Theorem 1:** For the Y channel composed of three single-antenna users and a two-antenna common access relay, the total DOF is upper bounded by 1.5, i.e.,

$$d \leq 1.5. \quad (5)$$

**Proof:** We first consider the network information flow from  $\{S_2, S_3\}$  to  $S_1$  as illustrated in **Fig. 2**. Using the fact that allowing cooperation of any two users among the three users does not reduce the DOF [11], we assume full cooperation between  $S_2$  and  $S_3$  to obtain an upper bound.

During the MAC phase (cut 2),  $S_2$  and  $S_3$  transmit signals to  $R$  simultaneously. We can treat the channel from  $S_2$  and  $S_3$  to  $R$  as a  $2 \times 2$  MIMO channel, whose DOF is well-known as  $\min\{2, 2\} = 2$ . Similarly, we can obtain the DOF of the channel in the BC phase (cut 1) as  $\min\{1, 2\} = 1$ . Applying the cut-set theorem in [27] to the two phases, the cut-set bound on DOF for the network information flow from  $\{S_2, S_3\}$  to  $S_1$  is obtained as

$$d_{1,2} + d_{1,3} \leq \frac{1}{2} \min\{2, 1\} = 0.5, \quad (6)$$

where the pre-log  $1/2$  is due to the fact that the transmission is completed in two time slots.

For the other two directions of the network information flow, i.e., messages from  $\{S_1, S_3\}$  to  $S_2$  and from  $\{S_1, S_2\}$  to  $S_3$ , we can get similar results as

$$d_{2,1} + d_{2,3} \leq 0.5, \quad (7)$$

$$d_{3,1} + d_{3,2} \leq 0.5. \quad (8)$$

Combining (6), (7), and (8), we obtain the total cut-set bound on DOF as

$$d = d_{1,2} + d_{1,3} + d_{2,1} + d_{2,3} + d_{3,1} + d_{3,2} \leq 1.5, \quad (9)$$

which completes the proof of the theorem.

#### 4. Achieving the Upper Bound: Asymmetric Signal Space Alignment

In this section, we describe the ASSA-based scheme in detail to prove the achievability of the DOF upper bound.

#### 4.1 Asymmetric Signal Space Alignment

According to [16], the relay and each user should have at least three and two antennas respectively to make SSA feasible for the considered scenario. In other words, traditional SSA scheme is not straightforwardly applicable when the system is lack of spatial dimension, i.e., each user is only equipped with one antenna. To this end, we first use ACS to convert the complex system into an equivalent real system with double dimensions. By employing the real-valued representation, we can rewrite (1) as

$$\tilde{\mathbf{y}}_R = \sum_{i=1}^3 \tilde{\mathbf{H}}_i \tilde{\mathbf{x}}_i + \tilde{\mathbf{n}}_R, \quad (10)$$

where the equivalent real-valued received signal is

$$\tilde{\mathbf{y}}_R = \left[ \text{Re}(y_{R_1}) \quad \text{Im}(y_{R_1}) \quad \text{Re}(y_{R_2}) \quad \text{Im}(y_{R_2}) \right]^T, \quad (11)$$

$y_{R_k}$  is the  $k$ th element of  $\mathbf{y}_R$ , the equivalent transmit signal is

$$\tilde{\mathbf{x}}_i = \left[ \text{Re}(x_i) \quad \text{Im}(x_i) \right]^T, \quad (12)$$

the equivalent noise is

$$\tilde{\mathbf{n}}_R = \left[ \text{Re}(n_{R_1}) \quad \text{Im}(n_{R_1}) \quad \text{Re}(n_{R_2}) \quad \text{Im}(n_{R_2}) \right]^T, \quad (13)$$

and  $n_{R_k}$  is the  $k$ th element of  $\mathbf{n}_R$ ,  $k \in \{1, 2\}$ . It is noted that the elements of  $\tilde{\mathbf{n}}_R$  are i.i.d. real Gaussian random variables following  $N(0, \sigma_R^2 / 2)$ . The real version of the channel matrix is expressed as

$$\tilde{\mathbf{H}}_i = \begin{bmatrix} \text{Re}(h_{i_1}) & -\text{Im}(h_{i_1}) \\ \text{Im}(h_{i_1}) & \text{Re}(h_{i_1}) \\ \text{Re}(h_{i_2}) & -\text{Im}(h_{i_2}) \\ \text{Im}(h_{i_2}) & \text{Re}(h_{i_2}) \end{bmatrix}, \quad (14)$$

where  $h_{i_k}$  is the  $k$ th element of  $\mathbf{h}_i$ ,  $k \in \{1, 2\}$ . Consequently, the  $2 \times 1$  complex channel  $\mathbf{h}_i$  for the link  $S_i \rightarrow R$  is transformed into the  $4 \times 2$  real matrix  $\tilde{\mathbf{H}}_i$ . In other words, the number of dimensions at all the nodes is doubled. In fact, the system always works as equation (1) in actual transmission. And the real-valued equation (10) is just an equivalent representation of the system, which is used to facilitate the beamforming design.

By employing the extra spatial dimensions introduced by the ACS, we design the transmit signal as

$$\tilde{\mathbf{x}}_i = \sum_{j=1, j \neq i}^3 \mathbf{v}_{j,i} d_{j,i}, \quad (15)$$

where  $d_{j,i} \in \mathbf{R}$  is the real scalar data from  $S_i$  to  $S_j$  with unit variance, and  $\mathbf{v}_{j,i} \in \mathbf{R}^{2 \times 1}$  denotes the corresponding precoding vector. To align each pair of signals into the same dimension, the paired precoding vectors  $\mathbf{v}_{j,i}$  and  $\mathbf{v}_{i,j}$  are designed to satisfy

$$\text{span}(\tilde{\mathbf{H}}_i \mathbf{v}_{j,i}) = \text{span}(\tilde{\mathbf{H}}_j \mathbf{v}_{i,j}). \quad (16)$$

This is equivalent to solving

$$\begin{bmatrix} \tilde{\mathbf{H}}_i & -\tilde{\mathbf{H}}_j \end{bmatrix} \begin{bmatrix} \mathbf{v}_{j,i} \\ \mathbf{v}_{i,j} \end{bmatrix} = \bar{\mathbf{H}}_l \bar{\mathbf{v}}_l = 0, \quad (17)$$

where the subscript  $l \in \{1, 2, 3\}$  is defined as the index of user pair  $\{S_i, S_j\}$  and  $l = \pi(i, j) = \pi(j, i)$ . More specifically, we define  $1 = \pi(1, 2)$ ,  $2 = \pi(1, 3)$ , and  $3 = \pi(2, 3)$ . However, since  $\bar{\mathbf{H}}_l \in \mathbf{R}^{4 \times 4}$  is a square matrix with full rank, its nullspace, which is also the intersection subspace of  $\text{span}(\tilde{\mathbf{H}}_i)$  and  $\text{span}(\tilde{\mathbf{H}}_j)$ , does not exist. As a result, we still cannot align each pair of signals.

In order to tackle the difficulty above, we carefully design a projection matrix at the relay. More specifically, we employ a projection matrix  $\mathbf{Q} \in \mathbf{R}^{4 \times 3}$  at the relay to change the size of the equivalent channel matrix. The columns of  $\mathbf{Q}$  are assumed to be orthonormal, i.e.,  $\mathbf{Q}^T \mathbf{Q} = \mathbf{I}$ . Specifically, we multiply the received signal with  $\mathbf{Q}^T$ . As a result, the problem in (17) is turned into

$$\mathbf{Q}^T \begin{bmatrix} \tilde{\mathbf{H}}_i & -\tilde{\mathbf{H}}_j \end{bmatrix} \begin{bmatrix} \mathbf{v}_{j,i} \\ \mathbf{v}_{i,j} \end{bmatrix} = \mathbf{Q}^T \bar{\mathbf{H}}_l \bar{\mathbf{v}}_l = 0. \quad (18)$$

Then we can obtain  $\bar{\mathbf{v}}_l$  from the nullspace of  $\mathbf{Q}^T \bar{\mathbf{H}}_l \in \mathbf{R}^{3 \times 4}$ . We assume equal power allocation for the two data streams of each user. As a result, in order to constrain the transmit power of each pair,  $\bar{\mathbf{v}}_l$  should satisfy  $\|\bar{\mathbf{v}}_l\|^2 = \|\mathbf{v}_{j,i}\|^2 + \|\mathbf{v}_{i,j}\|^2 \leq 0.5(P_i + P_j)$ . Consequently, we set  $\bar{\mathbf{v}}_l = \sqrt{0.5(P_i + P_j)} \check{\mathbf{v}}_l$ , where  $\check{\mathbf{v}}_l$  is a normalized vector in the nullspace of  $\mathbf{Q}^T \bar{\mathbf{H}}_l$ . We note that there is potential for optimizing  $\mathbf{Q}$  to improve the sum rate performance. The design of  $\mathbf{Q}$  will be discussed in section 5.

We define the equivalent MAC channel for each user pair as

$$\mathbf{Q}^T \tilde{\mathbf{H}}_i \mathbf{v}_{j,i} = \mathbf{Q}^T \tilde{\mathbf{H}}_j \mathbf{v}_{i,j} = \mathbf{u}_l. \quad (19)$$

As a result, the received signal processed by  $\mathbf{Q}^T$  at the relay can be presented as

$$\mathbf{Q}^T \tilde{\mathbf{y}}_R = \sum_{l=1}^3 \mathbf{u}_l d_{l+} + \mathbf{Q}^T \tilde{\mathbf{n}}_R, \quad (20)$$

where  $d_{l+} = d_{j,i} + d_{i,j}$  denotes the AF network coded message for the  $l$ th pair. It is indicated in (20) that the six signals are aligned into three dimensions. Consequently, linear receiver can be used at the relay to decouple the composite signals. In the BC phase, we also need to design each user's decoding vector to align the signal space of each pair. Only then can the relay perform linear precoding. Thanks to channel reciprocity, we can simply set the decoding vectors as  $\mathbf{w}_{i,j} = \mathbf{v}_{j,i}^T$ , which simplifies the computational complexity. For simplicity, we adopt zero-forcing (ZF) linear transceiver at the relay, which is designed as

$$\tilde{\mathbf{G}} = \mathbf{Q}(\mathbf{U}^T)^\dagger \mathbf{F} \mathbf{U} \mathbf{Q}^T, \quad (21)$$

where  $\mathbf{U} = [\mathbf{u}_1 \ \mathbf{u}_2 \ \mathbf{u}_3]$ ,  $\mathbf{u}_l$  is given in (19),  $\mathbf{F} = \text{diag}(f_1, f_2, f_3)$  is the power constraint matrix, and the diagonal elements are given as



$$f_l = \sqrt{\frac{\left( (\mathbf{U}^T \mathbf{U})_{l,l}^\dagger \right)^{-1} P_R}{6}}. \quad (22)$$

By utilizing  $\mathbf{F}$ , the long-term transmission power at the relay can be constrained as  $P_R$  [28].

**Remark:** In actual transmission, the relay first transforms the complex channel vector  $\mathbf{h}_i$  into real channel matrix  $\tilde{\mathbf{H}}_i$  as equation (14) and designs the beamforming vectors for each user as equation (18). Then the relay feeds back the beamforming vectors to the users. Finally, the users design the real signal according to equation (15) and transmit the signal in complex form as  $x_i = \tilde{\mathbf{x}}_{i_1} + \tilde{\mathbf{x}}_{i_2} j$ , where  $\tilde{\mathbf{x}}_k$ ,  $k=1, 2$  is the  $k$ th element of  $\tilde{\mathbf{x}}_i$ , and  $j$  is imaginary unit.

## 4.2 Brief DOF Evaluation

After applying decoding vector  $\mathbf{w}_{i,j} = \mathbf{v}_{j,i}^T$  and self-interference cancellation,  $S_i$  receives the signal as

$$\tilde{y}_{i,j} = \mathbf{v}_{j,i}^T (\tilde{\mathbf{H}}_i^T \tilde{\mathbf{x}}_R + \tilde{\mathbf{n}}_i) - f_l d_{j,i}. \quad (23)$$

By substituting (19), (20), and (21) into (23), we can rewrite (23) as

$$\tilde{y}_{i,j} = f_l d_{i,j} + \mathbf{F}_l \mathbf{U}^\dagger \mathbf{Q}^T \tilde{\mathbf{n}}_R + \mathbf{v}_{j,i}^T \tilde{\mathbf{n}}_i, \quad (24)$$

where  $\mathbf{F}_l$  is the  $l$ th row of  $\mathbf{F}$ . The end-to-end sum rate is calculated as

$$R = \frac{1}{2} \sum_{i=1}^3 \sum_{j=1, j \neq i}^3 \log(1 + \rho_{j,i}), \quad (25)$$

where the received SNR for the data stream from  $S_j$  to  $S_i$  is derived from (24) as follows

$$\rho_{i,j} = \frac{f_l^2}{\frac{N_0}{2} \times \left( \frac{P_R}{6} + \mathbf{v}_{j,i}^T \mathbf{v}_{j,i} \right)}, \quad (26)$$

and the pre-log  $1/2$  in (25) is due to the real signal. We can see that, after all the inter-pair and intra-pair interferences are eliminated, the desired signal is only contaminated by Gaussian noise. In other words, six real data streams are transmitted without interference within two time slots. According to [29], the DOF of one real symbol is 0.5. Consequently, the DOF achieved by the proposed ASSA scheme is

$$d_{\text{ASSA}} = \frac{6 \times 0.5}{2} = 1.5, \quad (27)$$

which is a lower bound of the DOF. Hence we obtain

$$d \geq d_{\text{ASSA}} = 1.5. \quad (28)$$

So far, we have obtained the DOF of the addressed Y channel. The main result is summarized in the following theorem.

**Theorem 2:** For the Y channel composed of three single-antenna users and a two-antenna common access relay, the total DOF is 1.5, i.e.,

$$d = 1.5. \quad (29)$$

**Proof:** Combining the upper bound in (5) and the lower bound in (28), we prove that the exact DOF of the channel model we investigate is 1.5.

**Remark:** The ASSA based scheme is not straightforwardly applicable to the scenario with

more than three users, where the beamforming design is rather challenging due to the insufficient dimensions of signal space. However, we can still make the proposed algorithm applicable in such cases by combining it with the user scheduling method proposed in [20].

## 5. Beamforming Optimization for ASSA

### 5.1 Iterative Joint Beamforming Optimization Algorithm

It is shown in (19), (22), (25), and (26) that the sum rate is a function of  $\mathbf{Q}$  and  $\mathbf{v}_{j,i}$ . This observation motivates us to study the beamforming optimization to further enhance the sum rate.

Because of the symmetrical beamforming design in MAC and BC phases, we follow [17] and only consider the MAC phase for simplicity. First, a mathematically equivalent expression of the ZF processing at the relay is presented. Specifically, instead of the pseudoinverse in (21), we use a unit norm vector  $\mathbf{p}_l \in \mathbf{R}^{3 \times 1}$  to extract the signal of the  $l$ th pair. According to [30], the optimal design of  $\mathbf{p}_l$  is given as  $\mathbf{p}_l = \langle \mathbf{M}_l \mathbf{u}_l \rangle$ , where

$$\mathbf{M}_l = \mathbf{I} - \hat{\mathbf{U}}_l \left( \hat{\mathbf{U}}_l^T \hat{\mathbf{U}}_l \right)^\dagger \hat{\mathbf{U}}_l^T, \quad (30)$$

and  $\hat{\mathbf{U}}_l$  is a submatrix of  $\mathbf{U}$  by removing its  $l$ th column  $\mathbf{u}_l$ . After the processing of  $\mathbf{p}_l$  and  $\mathbf{Q}$ , the signal of the  $l$ th pair is acquired as

$$\mathbf{p}_l^T \mathbf{Q}^T \tilde{\mathbf{y}}_R = \mathbf{p}_l^T \mathbf{u}_l d_{l+} + \mathbf{p}_l^T \mathbf{Q}^T \tilde{\mathbf{n}}_R. \quad (31)$$

After some derivations, the SNR for the  $l$ th pair is obtained as

$$\rho_l = \frac{2(P_i + P_j)}{\sigma_R^2} \mathbf{u}_l^T \mathbf{M}_l \mathbf{u}_l. \quad (32)$$

In order to maximize the sum rate, we formulate the beamforming design as the following joint optimization problem

$$\max_{\{\mathbf{v}_{j,i}, \mathbf{v}_{i,j}, \mathbf{Q}\}} R_{MAC} = \frac{1}{2} \sum_{l=1}^3 \log(1 + \rho_l) \quad (33)$$

$$\text{subject to } \mathbf{Q}^T \bar{\mathbf{H}}_l \begin{bmatrix} \mathbf{v}_{j,i} \\ \mathbf{v}_{i,j} \end{bmatrix} = 0, \quad (34)$$

$$\|\mathbf{v}_{j,i}\|^2 + \|\mathbf{v}_{i,j}\|^2 \leq 0.5(P_i + P_j), \quad (35)$$

$$\mathbf{Q}^T \mathbf{Q} = \mathbf{I}. \quad (36)$$

It is shown in (34) that  $\mathbf{Q}$  and  $\mathbf{v}_{j,i}$  are relevant, therefore we need to design them jointly. It is difficult to find the optimal solution because of the extremely high complexity. Therefore, the key issue is how to decouple these variables. We carefully study the coupling part of all the variables and introduce a unit-norm vector  $\mathbf{q}$  to express all the variables. More specifically, we assume  $\mathbf{Q}^T \mathbf{q} = 0$ . As a result, we can reformulate (34) as

$$\bar{\mathbf{H}}_l \begin{bmatrix} \mathbf{v}_{j,i} \\ \mathbf{v}_{i,j} \end{bmatrix} = \alpha_l \mathbf{q}, \quad (37)$$

where  $\alpha_l$  is used to meet the power constraint in (35). From (34), we can obtain

$$\begin{bmatrix} \mathbf{v}_{j,i} \\ \mathbf{v}_{i,j} \end{bmatrix} = \alpha_l \bar{\mathbf{H}}_l^\dagger \mathbf{q} = \alpha_l \begin{bmatrix} \mathbf{A}_{j,i} \\ \mathbf{A}_{i,j} \end{bmatrix} \mathbf{q}, \quad (38)$$

where  $\mathbf{A}_{j,i} \in \mathbf{R}^{2 \times 4}$  and  $\mathbf{A}_{i,j} \in \mathbf{R}^{2 \times 4}$  contain the first and last two rows of  $\bar{\mathbf{H}}_l^\dagger$ , respectively. Consequently, the precoding vectors can be written as

$$\mathbf{v}_{j,i} = \alpha_l \mathbf{A}_{j,i} \mathbf{q}, \quad (39)$$

$$\mathbf{v}_{i,j} = \alpha_l \mathbf{A}_{i,j} \mathbf{q}. \quad (40)$$

In order to control the transmit power, we let

$$\|\mathbf{v}_{j,i}\| = \alpha_l \|\mathbf{A}_{j,i} \mathbf{q}\| \leq \alpha_l \|\mathbf{A}_{j,i}\|_F \leq \sqrt{\frac{P_i}{2}}, \quad (41)$$

which results in  $\alpha_l \leq \sqrt{\frac{P_i}{2}} \|\mathbf{A}_{j,i}\|_F^{-1}$ . Similarly, we have  $\alpha_l \leq \sqrt{\frac{P_j}{2}} \|\mathbf{A}_{i,j}\|_F^{-1}$ . Hence, we assume

$$\alpha_l = \min \left\{ \sqrt{\frac{P_i}{2}} \|\mathbf{A}_{j,i}\|_F^{-1}, \sqrt{\frac{P_j}{2}} \|\mathbf{A}_{i,j}\|_F^{-1} \right\}. \quad (42)$$

Since the column space of  $\mathbf{q}$  is the orthogonal complement of that of  $\mathbf{Q}$ , we arrive at

$$\mathbf{Q}\mathbf{Q}^T = \mathbf{I} - \mathbf{q}\mathbf{q}^T. \quad (43)$$

By substituting (19), (30), (39), and (43) into (43), we get the SNR expression with  $\mathbf{q}$  as the only variable vector as follows

$$\begin{aligned} \rho_l = & \frac{2(P_i + P_j)}{\sigma_R^2} \left( \alpha_l^2 \mathbf{q}^T \mathbf{A}_{j,i}^T \tilde{\mathbf{H}}_i^T (\mathbf{I} - \mathbf{q}\mathbf{q}^T) \tilde{\mathbf{H}}_i \mathbf{A}_{j,i} \mathbf{q} - \alpha_l^2 \mathbf{q}^T \mathbf{A}_{j,i}^T \tilde{\mathbf{H}}_i^T (\mathbf{I} - \mathbf{q}\mathbf{q}^T) \right. \\ & \left. \begin{bmatrix} \alpha_m \tilde{\mathbf{H}}_a \mathbf{A}_{b,a} \mathbf{q} & \alpha_n \tilde{\mathbf{H}}_c \mathbf{A}_{d,c} \mathbf{q} \end{bmatrix} \begin{bmatrix} \alpha_m \tilde{\mathbf{H}}_a \mathbf{A}_{b,a} \mathbf{q} & \alpha_n \tilde{\mathbf{H}}_c \mathbf{A}_{d,c} \mathbf{q} \end{bmatrix}^T \right. \\ & \left. (\mathbf{I} - \mathbf{q}\mathbf{q}^T) \begin{bmatrix} \alpha_m \tilde{\mathbf{H}}_a \mathbf{A}_{b,a} \mathbf{q} & \alpha_n \tilde{\mathbf{H}}_c \mathbf{A}_{d,c} \mathbf{q} \end{bmatrix}^\dagger \right) \\ & \left. \begin{bmatrix} \alpha_m \tilde{\mathbf{H}}_a \mathbf{A}_{b,a} \mathbf{q} & \alpha_n \tilde{\mathbf{H}}_c \mathbf{A}_{d,c} \mathbf{q} \end{bmatrix}^T (\mathbf{I} - \mathbf{q}\mathbf{q}^T) \tilde{\mathbf{H}}_i \mathbf{A}_{j,i} \mathbf{q} \right), \end{aligned} \quad (44)$$

where the subscript  $a, b, c, d \in \{1, 2, 3\}$ ,  $m = \pi(a, b)$ ,  $n = \pi(c, d)$ ,  $m \neq n$ ,  $l \neq m$ , and  $l \neq n$ . And the optimization problem is simplified as

$$\max_{\{\mathbf{q}\}} R_{MAC} = \frac{1}{2} \sum_{l=1}^3 \log(1 + \rho_l) \quad (45)$$

$$\text{subject to } \|\mathbf{q}\| = 1. \quad (46)$$

However, the above optimization problem is non-convex with respect to  $\mathbf{q}$  [26], so it is still difficult to find the optimal solution. We obtain a local solution iteratively by using the combination of penalty function method and quasi-Newton method, which is effective to solve the equality constrained optimization problem [26]. Initially, we employ penalty function method to convert the problem in (45) into an unconstrained problem as

$$\min_{\{\mathbf{q}\}} g(\mathbf{q}) = -f(\mathbf{q}) + \mu h(\mathbf{q}), \quad (47)$$

where

$$f(\mathbf{q}) = \frac{1}{2} \sum_{l=1}^3 \log(1 + \rho_l) \quad (48)$$

is the original objective function,  $h(\mathbf{q}) = (\mathbf{q}^T \mathbf{q} - 1)^2$  is the penalty function and  $\mu > 0$  is the penalty coefficient. Next, the quasi-Newton method is used to solve the problem in (47). Once  $\mathbf{q}$  is obtained, we can calculate  $\mathbf{v}_{j,i}$  and  $\mathbf{Q}$  according to (39), (40), and (43). The detail of I-JBO algorithm is summarized in **Table 1**. Although we cannot guarantee that the proposed iterative algorithm converges to the global optimal solution due to the nonconvexity of the objective function, we can still demonstrate the sum rate enhancement via numerical results. (See section 6 for details.)

**Table 1.** Iterative joint beamforming optimization algorithm

<p><b>Initialization step:</b>  <math>k_{p \max} = 10</math>: the maximum number of iterations for penalty function method  <math>k_{n \max} = 100</math>: the maximum number of iterations for quasi-Newton method  <math>\varepsilon_p = 0.01</math>: the threshold for terminating penalty function method  <math>\varepsilon_n = 0.001</math>: the threshold for terminating quasi-Newton method  <math>\beta = 10</math>: the multiple coefficient of <math>\mu</math></p>
<p><b>Main step:</b>  Initialize <math>\mathbf{q}_1 = [1 \ 0 \ 0 \ 0]^T</math>, <math>\mathbf{D}_1 = \mathbf{I}_{4 \times 4}</math> and <math>\mu_1 = 1</math>  <b>for</b> <math>k = 1 : k_{p \max}</math>    Initialize <math>\mathbf{q}'_1 = \mathbf{q}_k</math>, <math>j = 1</math> and <math>i = 1</math>    <b>while</b> <math>j \leq 4</math> (The dimension of <math>\mathbf{q}</math> is 4)      <b>If</b> <math>\ \nabla g(\mathbf{q}'_j)\  &lt; \varepsilon_n</math> or <math>i &gt; k_{n \max}</math> (<math>\nabla g(\mathbf{q})</math> is the gradient of <math>g(\mathbf{q})</math>)        break      <b>else</b>        <math>\mathbf{d}_j = -\mathbf{D}_j \nabla g(\mathbf{q}'_j)</math>        Find <math>\lambda_j \geq 0</math> to minimize <math>g(\mathbf{q}'_j + \lambda_j \mathbf{d}_j)</math>        Update <math>\mathbf{q}'_{j+1} = \mathbf{q}'_j + \lambda_j \mathbf{d}_j</math>        <b>If</b> <math>j &lt; 4</math>          <math>\mathbf{b}_j = \mathbf{q}'_{j+1} - \mathbf{q}'_j</math>, <math>\mathbf{a}_j = \nabla g(\mathbf{q}'_{j+1}) - \nabla g(\mathbf{q}'_j)</math>          Update <math>\mathbf{D}_{j+1} = \mathbf{D}_j + \frac{\mathbf{b}_j \mathbf{b}_j^T}{\mathbf{b}_j^T \mathbf{a}_j} - \frac{\mathbf{D}_j \mathbf{a}_j \mathbf{a}_j^T \mathbf{D}_j}{\mathbf{a}_j^T \mathbf{D}_j \mathbf{a}_j}</math>          <math>j++</math>        <b>else</b>          Update <math>\mathbf{q}_{k+1} = \mathbf{q}'_{j+1}</math> and <math>j = 1</math>        <b>end</b>      <b>end</b>      <math>i++</math>    <b>end</b>  <b>If</b> <math>\mu_k h(\mathbf{q}_{k+1}) &lt; \varepsilon_p</math></p>

```

    break
  else
    Update  $\mu_{k+1} = \beta\mu_k$ 
  end
end
end

```

## 5.2 Evaluation of Computation Complexity

In this subsection, we discuss the computation complexity of the proposed beamforming optimization scheme along with the random beamforming design scheme as follows. We measure the complexity of the algorithms by counting the number of floating-point operations (flops).

We note that the calculation of  $\nabla g(\mathbf{q})$  takes most of the flops, so we focus on it and omit the other operations.  $\nabla g(\mathbf{q})$  can be calculated with a great number of applications of the product and quotient rules. However, the calculation process is tediously long, so we omit the calculation details here due to space limitation. Totally the flops of the proposed I-JBO algorithm is about  $K \times I \times 2.11 \times 10^5$ , where  $K$  and  $I$  are the number of iterations in the outer loop and the inner loop respectively. The number of iterations in the inner loop may vary in every outer loop, so  $I$  is an average value. For comparison, we also count the flops of the random beam design, and the result is about  $3.85 \times 10^3$ . Although the proposed algorithm takes more computations, it can improve the sum rate significantly.

## 6. Numerical Results

In this section, we provide the numerical results to show the end to end sum rate performance of the proposed schemes, namely the ASSA transmission scheme, and the affiliated I-JBO beam design algorithm. In all the simulations, the i.i.d. Rayleigh flat fading channels are assumed. For fairness, we set  $P_i = P_r = P$  and  $\sigma_i^2 = \sigma_r^2 = N_0$  for all the test cases, so that the system transmit SNR becomes  $\rho = P/N_0$ . The sum rate in one channel realization is calculated according to (25). After that it is averaged from  $10^4$  channel realizations to get the ergodic sum rate. The convergence property of the I-JBO algorithm is also verified. More specifically, mean squared error (MSE) of the variable vector  $\mathbf{q}$  and the average value of the objective function are verified for both of the inner loop and outer loop.

At first, we compare the sum rate between the naive ZF in [31] and ASSA with different beam designs. Based on the definition of DOF, we set the x-axis as  $\log(\rho)$ , then the slope of the sum rate curve at high SNR represents the achievable DOF. Moreover, we also plot two straight lines with slope of 1 and 1.5 as references to verify the DOF results. As shown in Fig. 3, the curves that denote the ASSA with different beamforming designs, i.e., the red, green, and blue ones, all become parallel with the straight line with slope of 1.5 as SNR increases, which means the DOF of 1.5 is achieved. Similarly, we can easily read from the figure that the achieved DOF of the naive ZF scheme is 1. It is further illustrated that the performance of the iterative scheme in [17] is the same with the random beam design. The main reason is that the dimension of the intersection space of each user pair is one in the channel model we consider, consequently there is no room for the strategy proposed in [17] to optimize the beamforming. Especially at low-to-moderate SNR regime, the ASSA with iterative and random beam designs even perform worse than the naive ZF. This is because the transmission schemes

based on IA or SSA share one disadvantage, i.e., performing poorly at low SNR regime. Hence, although achieving higher DOF, it performs more poorly than the naive ZF scheme at low SNR regime. On the contrary, it is demonstrated that the I-JBO algorithm remarkably boosts the sum rate and achieves the best performance at almost all SNR regimes.

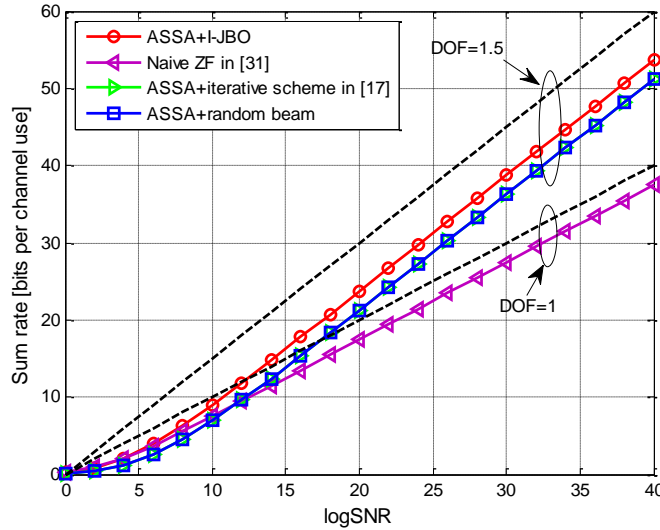


**Fig. 3.** Sum rate comparison between naive ZF and ASSA with different beamforming designs.

As shown in **Fig. 4**, the MSE of  $\mathbf{q}$  in the inner loop, i.e., quasi-Newton method, decreases to zero as the number of iterations increases. The MSE denotes the average distance between the variable obtained in each iteration and the final value. Therefore, the results mean the inner loop is capable of converging after a certain number of iterations. By comparing the black and green lines (or the blue and red ones), we can see that more iterations are required as the penalty coefficient  $\mu$  gets larger. On the contrary, fewer iterations are required as the SNR increases. Similar results can be seen in **Fig. 5**, which prove the convergence of the outer loop.

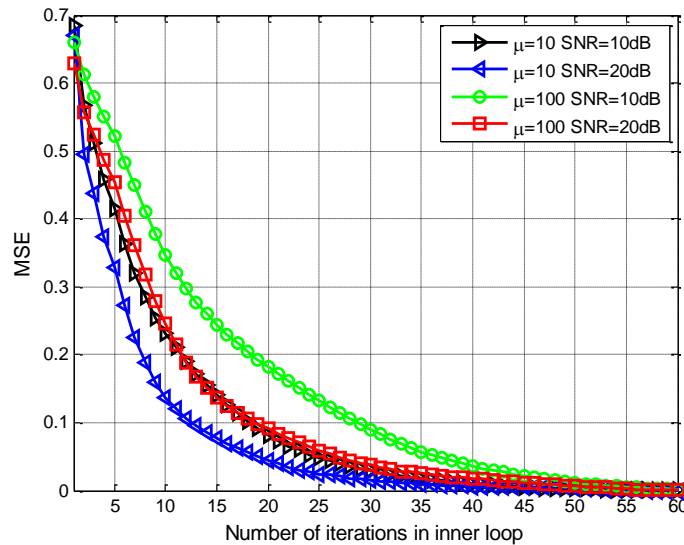


**Fig. 4.** The MSE of  $\mathbf{q}$  versus the number of iterations in the inner loop.

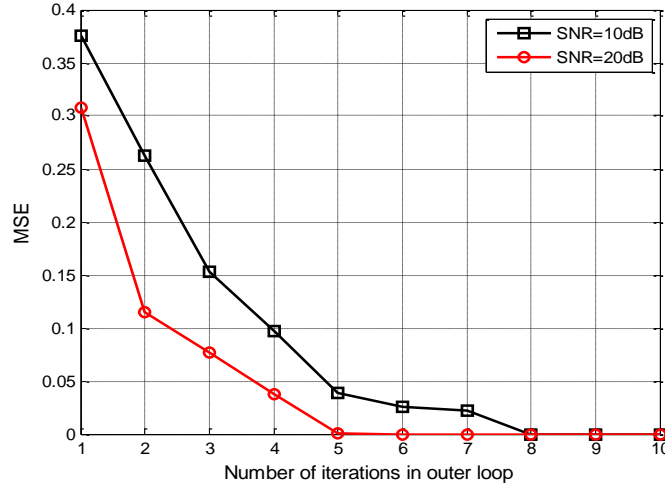


Fig. 5. The MSE of  $\mathbf{q}$  versus the number of iterations in the outer loop.

We also plot the average value of the objective function versus the number of iterations. The objective function for the inner loop is in equation (47). As shown in Fig. 6, the average value of the objective function decreases as the number of iterations increases and gets saturated after a certain number of iterations. Moreover, the inner loop converges more slowly as increases. On the contrary, higher SNR makes the loop converge faster. These results are quite consistent with the ones in Fig. 4. Meanwhile, we plot Fig. 7 to prove the convergence of the outer loop from the perspective of objective function value, where the objective function is shown in equation (45). We can see from Fig. 7 that the average value of the objective function also decreases as the number of iterations increases and converges after a few iterations. It is noted that our target is to maximize the objective function, i.e., sum rate, in equation (45). However, it is shown in Fig. 7 that the average value of the objective function decreases as the number of iterations increases. The reason is that although the vector  $\mathbf{q}$  obtained in the first few iterations can make the value of the objective function large, it may not satisfy the constraint  $\|\mathbf{q}\|=1$ , which makes the termination condition of the outer loop  $\mu_k h(\mathbf{q}_{k+1}) < \varepsilon_p$  false. As a result, the vector  $\mathbf{q}$  is returned back to the inner loop to get a new value until the termination condition holds.

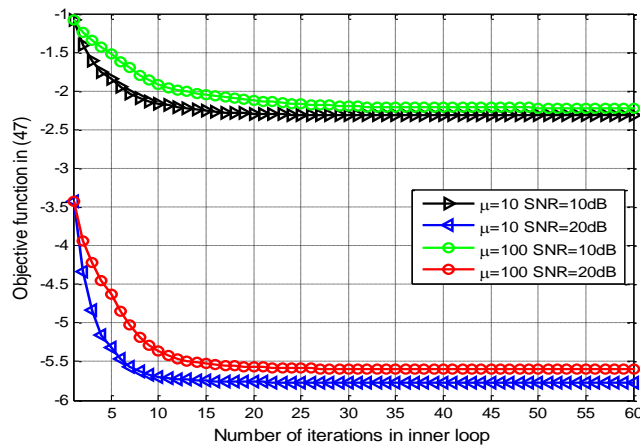


Fig. 6. The objective function in (47) versus the number of iterations in the inner loop.

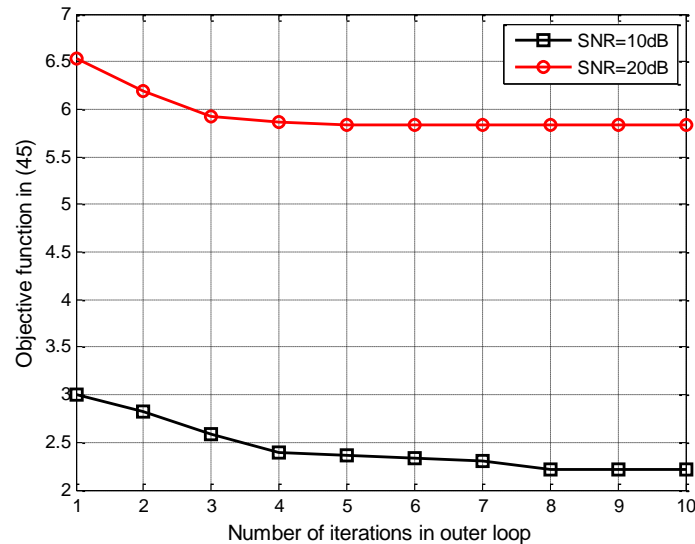


Fig. 7. The objective function in (45) versus the number of iterations in the outer loop.

## 7. Conclusion

In this paper, we investigate the DOF of the Y channel composed of three single-antenna users and a two-antenna common access relay, where each user intends to exchange independent messages with the other two users with the help of the relay. Initially, a DOF upper bound for this particular scenario is derived based on cut-set bound by allowing user cooperation, which shows that the total DOF is upper bounded by 1.5. To achieve the cut-set bound, we introduce the ASSA-based scheme. By using ACS to convert the complex system into an equivalent real system, more dimensions can be utilized for beamforming. Moreover, a projection matrix is utilized at the relay to enable the ASSA. Brief analysis and simulation results demonstrate that the proposed signaling technique achieves the DOF cut-set bound. Combining the upper bound and achievability, we conclude that the DOF of the channel model we study is 1.5. Furthermore, we also come up with the I-JBO beam design algorithm to further enhance the sum rate of the ASSA scheme. It is an interesting future topic to investigate the extension of our work into a general Y channel where there are arbitrary number of users and antennas.

## References

- [1] Z. Xu, W. Qin, Q. Tang, and D. Jiang, "Energy-efficient cognitive access approach to convergence communications," *SCIENCE CHINA Information Sciences*, vol. 57, pp. 1-12, 2014.  
[Article \(CrossRef Link\)](#).
- [2] R. Keralapura, A. Nucci, Z. L. Zhang, and L. Zhang, "Profiling users in a 3G network using hourglass co-clustering," in *Proc. of the ACM MobiCom*, pp. 341-351, 2010.  
[Article \(CrossRef Link\)](#).
- [3] D. Jiang, Z. Xu, P. Zhang, and T. Zhu, "A transform domain-based anomaly detection approach to network-wide traffic," *Journal of Network and Computer Applications*, vol. 40, pp. 292-306, 2014.  
[Article \(CrossRef Link\)](#).
- [4] H. Cao, J. Li, X. Fang, and X. Wang, "A novel pre-processing and adaptive statistical threshold for sphere detection in MIMO systems," *EURASIP Journal on Wireless Communications and*



- Networking*, vol. 275, pp. 1-8, 2013. [Article \(CrossRef Link\)](#).
- [5] “Partial Relay Selection in Decode and Forward Cooperative Cognitive Radio Networks over Rayleigh Fading Channels,” *KSII Transactions on Internet and Information Systems*, Accept.
- [6] C. Chai and C. Yuen, “On two-way communications for cooperative multiple source pairs through a multi-antenna relay,” in *Proc. of the Asilomar Conference on Signals, Systems, and Computers*, Pacific Grove, 2010, pp. 908–912. [Article \(CrossRef Link\)](#).
- [7] H. Gao, T. Lv, S. Zhang, C. Yuen, and S. Yang, “Zero-forcing based MIMO two-way relay with relay antenna selection: Transmission scheme and diversity analysis,” *IEEE Transactions on Wireless Communications*, vol. 11, pp. 4426–4437, Dec. 2012. [Article \(CrossRef Link\)](#).
- [8] Z. Fan, K. Xu, B. Zhang, and X. Pan, “Performance analysis of amplify-and-forward two-way relaying with antenna correlation,” *KSII Transactions on Internet and Information Systems*, vol. 6, no. 6, pp. 1606–1626, June 2012. [Article \(CrossRef Link\)](#).
- [9] S. Lou and L. Yang, “Opportunistic multiple relay selection for two-way relay networks with outdated channel state information,” *KSII Transactions on Internet and Information Systems*, vol. 8, no. 2, pp. 389–405, Feb. 2014. [Article \(CrossRef Link\)](#).
- [10] D. Gunduz, A. Yener, A. Goldsmith, and H. V. Poor, “The multiway relay channel,” *IEEE Transactions on Information Theory*, vol. 59, pp. 51–63, 2012. [Article \(CrossRef Link\)](#).
- [11] N. Lee, J. B. Lim, and J. Chun, “Degrees of freedom of the MIMO Y channel: Signal space alignment for network coding,” *IEEE Transactions on Information Theory*, vol. 56, pp. 3332–3342, 2010. [Article \(CrossRef Link\)](#).
- [12] S. A. Jafar and S. Shamai, “Degrees of freedom region of the MIMO X channel,” *IEEE Transactions on Information Theory*, vol. 54, pp. 151–170, 2008. [Article \(CrossRef Link\)](#).
- [13] S. Katti, S. Gollakota, and D. Katabi, “Embracing wireless interference: analog network coding,” in *Proc. of the ACM SIGCOMM*, Kyoto, 2007, pp. 397–408. [Article \(CrossRef Link\)](#).
- [14] S. Zhang, S. C. Liew, and L. Lu, “Physical layer network coding schemes over finite and infinite fields,” in *Proc. of the IEEE GLOBECOM*, New Orleans, 2008, pp. 1–6. [Article \(CrossRef Link\)](#).
- [15] B. Yuan, X. Liao, F. Gao, and X. Luo, “Achievable degrees of freedom of the four-user MIMO Y channel,” *IEEE Communications Letters*, vol. PP, pp. 1–4, 2013. [Article \(CrossRef Link\)](#).
- [16] K. Lee, N. Lee, and I. Lee, “Achievable degrees of freedom on K-user Y channels,” *IEEE Transactions on Wireless Communications*, vol. 11, pp. 1210–1219, 2012. [Article \(CrossRef Link\)](#).
- [17] Z. Zhou and B. Vucetic, “An iterative beamforming optimization algorithm for generalized MIMO Y channels,” in *Proc. of the IEEE ICC*, Ottawa, 2012, pp. 1–5. [Article \(CrossRef Link\)](#).
- [18] —, “Beamforming optimization for generalized MIMO Y channels with both multiplexing and diversity,” in *Proc. of the IEEE VTC*, Yokohama, 2012, pp. 1–5. [Article \(CrossRef Link\)](#).
- [19] N. Wang, Z. Ding, X. Dai, and A. V. Vasilakos, “On generalized MIMO Y channels: Precoding design, mapping, and diversity gain,” *IEEE Transactions on Vehicular Technology*, vol. 60, pp. 3525–3532, 2011. [Article \(CrossRef Link\)](#).
- [20] H. Gao, C. Yuen, H. A. Suraweera, and T. Lv, “Multiuser diversity for MIMO-Y channel: Max-min selection and diversity analysis,” in *Proc. of the IEEE ICC*, Budapest, 2013, pp. 5786–5791. [Article \(CrossRef Link\)](#).
- [21] A. Chaaban, A. Sezgin, and A. S. Avestimehr, “Approximate sum-capacity of the Y-channel,” *IEEE Transactions on Information Theory*, vol. 59, pp. 5723–5740, 2013. [Article \(CrossRef Link\)](#).
- [22] X. Zhang, Y. Xia, and S. Luo, “Energy-aware management in wireless body area network system,” *KSII Transactions on Internet and Information Systems*, vol. 7, no. 5, pp. 949–966, May 2013. [Article \(CrossRef Link\)](#).
- [23] R. Sheikhpour and S. Jabbehdari, “An energy efficient chain-based routing protocol for wireless sensor networks,” *KSII Transactions on Internet and Information Systems*, vol. 7, no. 6, pp. 1357–1378, June 2013. [Article \(CrossRef Link\)](#).
- [24] V. R. Cadambe, S. A. Jafar, and C. Wang, “Interference alignment with asymmetric complex signaling: Settling the høst-madsen–nosratinia conjecture,” *IEEE Transactions on Information Theory*, vol. 56, pp. 4552–4565, 2010. [Article \(CrossRef Link\)](#).

- [25] W. Long, T. Lv, H. Gao, Y. Lu, and E. Liu, "Asymmetric signal space alignment for Y channel with single-antenna users," in *Proc. of the IEEE ICC*, Budapest, Hungary, Jun. 2013, pp. 4834–4838. [Article \(CrossRef Link\)](#).
- [26] M. S. Bazaraa, H. D. Sherali, and C. M. Shetty, *Nonlinear Programming: Theory and Algorithms*, 3rd ed. Wiley, 2006. [Article \(CrossRef Link\)](#).
- [27] T. Cover and A. Gamal, "Capacity theorems for the relay channel," *IEEE Transactions on Information Theory*, vol. 25, pp. 572–584, 1979. [Article \(CrossRef Link\)](#).
- [28] Z. Ding, I. Krikidis, J. Thompson, and K. K. Leung, "Physical layer network coding and precoding for the two-way relay channel in cellular systems," *IEEE Transactions on Signal Processing*, vol. 59, pp. 696–712, 2011. [Article \(CrossRef Link\)](#).
- [29] A. S. Motahari, S. O. Gharan, M. A. Maddah-Ali, and A. K. Khandani, "Real interference alignment: Exploiting the potential of single antenna systems," *IEEE Transactions on Information Theory*, vol. 60, pp. 4799–4810, 2014. [Article \(CrossRef Link\)](#).
- [30] Z. Zhou and B. Vucetic, "An orthogonal projection optimization algorithm for multi-user MIMO channels," in *Proc. of the IEEE VTC*, Taipei, 2010, pp. 1–5. [Article \(CrossRef Link\)](#).
- [31] U. T. Amah and A. Klein, "Regenerative multi-group multi-way relaying," *IEEE Transactions on Vehicular Technology*, vol. 60, pp. 3017–302, 2011. [Article \(CrossRef Link\)](#).



**Wei Long** received his B.Eng. degree in information engineering from Beijing University of Posts and Telecommunications (BUPT), Beijing, China, in July 2008. He is now working towards the Ph.D. degree in the same school. His research interests focus on interference alignment and signal processing techniques in MIMO relay systems.



**Hui Gao** received his B. Eng. degree in Information Engineering and Ph.D. degree in Signal and Information Processing from Beijing University of Posts and Telecommunications (BUPT), Beijing, China, in July 2007 and July 2012, respectively. From May 2009 to June 2012, he also served as a research assistant for the Wireless and Mobile Communications Technology R&D Center, Tsinghua University, Beijing, China. From Apr. 2012 to June 2012, he visited Singapore University of Technology and Design (SUTD), Singapore, as a research assistant. From July 2012 to Feb. 2014, he was a Postdoc Researcher with SUTD. He is now with the School of Information and Communication Engineering, Beijing University of Posts and Telecommunications (BUPT), as an assistant professor. His research interests include massive MIMO systems, cooperative communications, ultra-wideband wireless communications.



**Tiejun Lv** received the M.S. and Ph.D. degrees in electronic engineering from the University of Electronic Science and Technology of China (UESTC), Chengdu, China, in 1997 and 2000, respectively. From January 2001 to December 2002, he was a Postdoctoral Fellow with Tsinghua University, Beijing, China. From September 2008 to March 2009, he was a Visiting Professor with the Department of Electrical Engineering, Stanford University, Stanford, CA. He is currently a Full Professor with the School of Information and Communication Engineering, Beijing University of Posts and Telecommunications (BUPT). He is the author of more than 100 published technical papers on the physical layer of wireless mobile communications. His current research interests include signal processing, communications theory and networking. Dr. Lv is also a Senior Member of the Chinese Electronics Association. He was the recipient of the Program for New Century Excellent Talents in University Award from the Ministry of Education, China, in 2006.



**Chau Yuen** received the B. Eng and PhD degree from Nanyang Technological University, Singapore in 2000 and 2004 respectively. Dr Yuen was a Post Doc Fellow in Lucent Technologies Bell Labs, Murray Hill during 2005. He was a Visiting Assistant Professor of Hong Kong Polytechnic University in 2008. During the period of 2006-2010, he worked at the Institute for Infocomm Research (Singapore) as a Senior Research Engineer. He joined Singapore University of Technology and Design as an assistant professor from June 2010. He serves as an Associate Editor for IEEE Transactions on Vehicular Technology. On 2012, he received IEEE Asia-Pacific Outstanding Young Researcher Award.